We are IntechOpen, the world's leading publisher of Open Access books
Built by scientists, for scientists

6,900
Open access books available

186,000
International authors and editors

200M
Downloads

Our authors are among the

154
Countries delivered to

TOP 1%
most cited scientists

12.2%
Contributors from top 500 universities

CLARIVATE ANALYTICS
BOOK CITATION INDEX
INDEXED

WEB OF SCIENCE™

Selection of our books indexed in the Book Citation Index
in Web of Science™ Core Collection (BKCI)

Interested in publishing with us?
Contact book.department@intechopen.com

Numbers displayed above are based on latest data collected.
For more information visit www.intechopen.com

Biocomposite Cement-Based Mortar

Xiaoniu Yu and Yan Gao

Additional information is available at the end of the chapter

Abstract

This chapter presents the preparation of a new kind of biocement based on the biophosphate minerals, which have cementation, by the bacteria reacting with the substrate. Ammonia/ammonium can be changed into environment-friendly struvite when the soluble phosphate is added to biocarbonate cement. After that, struvite and carbonate, which can be considered as composite cements, are applied to cement loose particles. The biocement is environmentally friendly, which has important application prospects. Based on mixing-precipitation process, the injection process was adopted to bind loose sand particles. Permeability, porosity, compressive strength, and internal microstructure of the biosandstones cemented by composite cement were determined under different number of injections. Mixing-precipitation process was inferior to injection process according to compressive strength of the biosandstones caused by the particle size and morphology of composite cement. Permeability, porosity, compressive strength, and fixation ammonia ratio of the biosandstones were compared when three different formulations of composite cement (CJ1, CJ1.5, and CJ2) were adopted to bind sand columns. The results show that the CJ2 has the best overall performance. The molar ratio of $K_2HPO_4 \cdot 3H_2O$ and urea was 2:1 in the CJ2 formulation.

Keywords: biocement, struvite, carbonate, bind, sand particles, injection process, compressive strength, sand columns

1. Introduction

Portland cement is the most commonly used cementing material in the construction field and an important part of the building materials industry. The main raw material of cement is limestone. During the production process, limestone is burned with fossil fuels, and the greenhouse gas CO_2 is decomposed and released. When the fuel is burned, harmful gases such as SO_2 and NO_x are also emitted, causing adverse effects on the ecological and

environmental systems. Based on microbial cement, it can consolidate loose particles with low energy consumption and less pollution. It can solve some disadvantages of traditional materials in the fields of ground reinforcement, desert treatment, dust control, etc. Biocement, based on microbial-induced mineralization, can consolidate the loose particles and would be a novel and sustainable cementing material which is applied to foundation reinforcement, dust control, and other fields.

The biocalcite cement, as one kind of biocement, has been investigated widely [1–6]. However, ammonia will be released in the cementation process of biocalcite cement, which has a negative impact on the ecological environment. It is a new type of sustainable development of cementitious materials. Biocarbonate cement can be used to cement loose grains into a whole with good mechanical properties through a grouting process. The main purpose of this chapter is to convert the ammonia/ammonium released from urease hydrolysis of urea into environmentally friendly struvite during the cementation process, and cemented loose particles together with carbonates. This can partially replace the chemical grouting materials commonly used in the treatment of foundations today, such as cement pastes, water glass, epoxy resins, methacrylates, polyurethanes, acrylic amines, lignin, and other chemical reinforcement materials. The biocomposite cement is injected into the prepared quartz sand mold through a peristaltic pump, and the loose particles can be cemented well into a whole with mechanical properties, and the ammonia/ammonium produced during the cementation of the biocarbonate cement can be converted into environmentally friendly struvite. The mineralization reaction of the cement in the pores between the loose particles produces struvite and hydromagnesite composite cementitious materials, which can improve the permeability, pore structure, and mechanical properties of the sand.

2. Biocomposite cement bind sand process

2.1. Preprecipitation mixing process molding sand columns

2.1.1. Biocomposite cement slurry with different standing time molding sand columns by preprecipitation mixing process

About 4 mol of $K_2HPO_4 \cdot 3H_2O$ was completely dissolved in the carbonate-mineralized bacteria (*Sporosarcina pasteurii*, 2 L), for CJ2. Divided into 18, 100 mL each, 1 group for 3 samples. Then, 100 mL of urea (1 mol/L) and $MgCl_2$ (3 mol/L) were sequentially added to obtain a precipitated solution. The settling solution was left standing every three groups for 0, 2, 6, 12, 24, and 40 h. The supernatant was removed, each group of sediment (30% of the total sand column) was mixed with quartz sand (particle size 425–212 μm), mechanically mixed until uniform, and the mixture was poured into a plastic mold (Φ 3cm × 6 cm), as shown in **Figure 1**. The molded specimens were placed in a 30 ± 2°C oven for drying. The molds were removed and the corresponding sand columns were obtained.

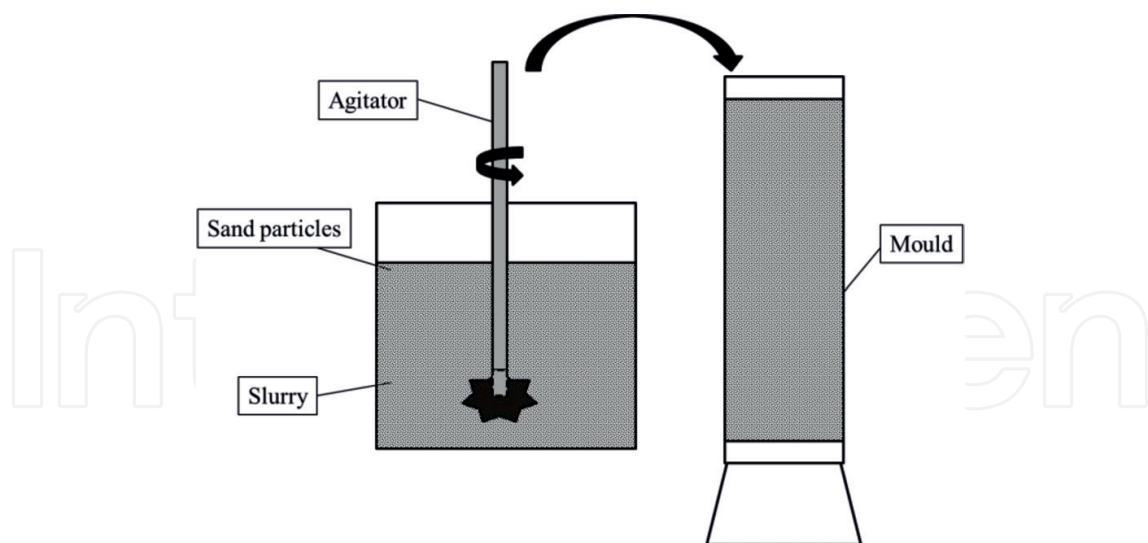**Figure 1.** Schematic diagram of the preprecipitation mixing process.

Standing time (h)	0	2	6	12	24	40
Compressive strength (MPa)	0.18	0.42	0.38	0.34	0.34	0.21

Table 1. Effect of standing time of precipitated slurry on the average compressive strength of the biosandstones.

The average compressive strength of the sand column is shown in **Table 1**, which are 0.18, 0.42, 0.38, 0.34, 0.34, and 0.21 MPa, respectively. The average compressive strength of the bio-BaHPO$_4$ slurry (30% of the total sand column) cement sand column (Φ 3cm × 6 cm) is 0.90 MPa [1]. The results show that the average compressive strength of sand columns cemented by the composite cement slurry in mixing process is lower than that of the bio-BaHPO$_4$ slurry.

2.1.2. Different contents of biocomposite cement slurry forming sand column by preprecipitation mixing process

The raw file of the composite cement slurry (standing time for 6 h) was analyzed by the MDI Jade 5.0 program. The results showed that the composition of the product was the mixture of $MgNH_4PO_4 \cdot 6H_2O$ (JCPDS No. 03-0240) (JCPDS No. 03-0240) and $Mg_5(CO_3)_4(OH)_2(H_2O)_4$ (JCPDS No. 70-1177) (**Figure 2**). SEM images show that the morphology of the mixture is irregular, the surface is relatively rough, and the particle size is in the range of 150–500 μm, as shown in **Figure 3**.

The average compressive strength of the sand columns (Φ 3cm × 6 cm) cemented 10, 20, 30, 40, 50, and 60% for the composite cement slurry (standing time for 6 h) were 0.13, 0.25, 0.38, 0.36, 0.35, and 0.36 MPa, respectively, as shown in **Table 2**. Compared with the average compressive
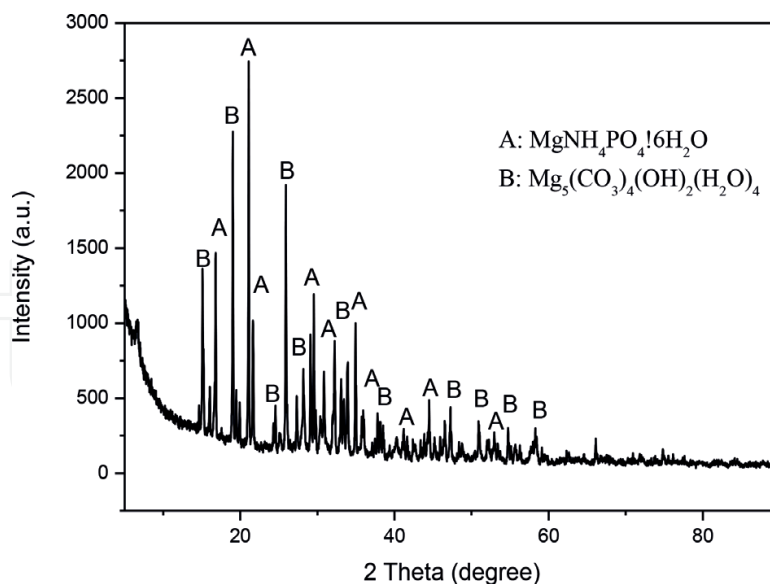
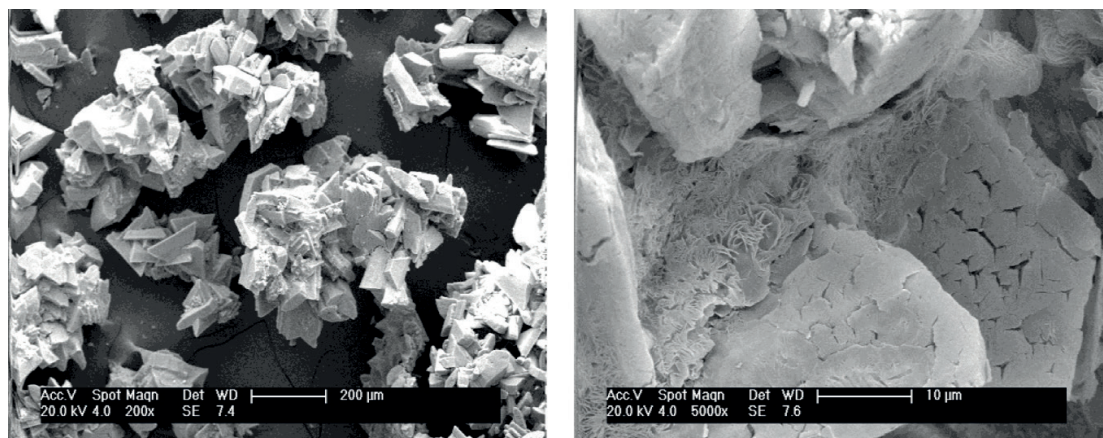**Figure 2.** XRD patterns of the precipitated slurry.

Figure 3. SEM images of the precipitated slurry.

strength of sand columns (Φ 3cm × 6 cm) cemented bio-$BaHPO_4$ slurry at different dosages, the average compressive strength of sand columns cemented by composite cement slurry is lower [7]. Therefore, the grouting process was used to cement the loose sand.

2.2. Biogrouting process forming sand columns

Quartz sand with different particle sizes (particle diameter 425–212 μm) was mechanically mixed until uniform. CJ1 represents per liter of carbonate-mineralized bacteria containing 1 mol of $K_2HPO_4 \cdot 3H_2O$. Before adding loose sands, put a 1.0-mm high gauze on the bottom of the PVC pipe (Φ 5cm × 15 cm), then place sands in a PVC pipe and compact it to dense. Finally, put a 1.0-mm high gauze on top of PVC pipe. The bottom of the PVC tube (the bottom of the cylinder) was connected with a peristaltic pump that the flow rate can be regulated, and

Content (%)	10	20	30	40	50	60
Compressive strength (MPa)	0.13	0.25	0.38	0.36	0.35	0.36

Table 2. Effect of content of composite cement slurry on the average compressive strength of the biosandstones.

inject the solution from the bottom to top. The steps are as follows: (1) injecting tap water into the mold at a flow rate of 16 mL/min to eliminate air bubbles existing between the particles; (2) injecting 100 mL of CJ1; (3) injecting 100 mL of (1 mol/L) urea and (2 mol/L) $MgCl_2$ mixed solution and stand for 6 h; (4) injecting 100 mL of CJ1 and allowed to stand for 6 h; (5) 100 mL of (1 mol/L) urea and (2 mol/L) $MgCl_2$ mixed solution was injected and allowed to stand for 6 h; (6) 100 mL of CJ1 was injected and allowed to stand for 6 h, and so on, until unable to inject CJ1 and urea and $MgCl_2$ of mixed solution to sand columns. Then, the samples with the mold were placed in an oven ($30 \pm 2°C$) to dry for 21 days, and then the mold was removed. All experiments were performed in triplicate and cemented at $30 \pm 2°C$. The number of injections of CJ1 was 2, 4, and 6, respectively (**Figure 4**).

2.2.1. XRD pattern of sand columns

The constituents of the sand column were analyzed through XRD, as shown in **Figure 5**. The sand column components were mainly a mixture of quartz sand (JCPDS No. 46-1045), $MgNH_4PO_4(H_2O)_6$ (JCPDS No. 71-2089), and $Mg_5(CO_3)_4(OH)_2 \cdot 4H_2O$ (JCPDS No. 25-0513). The XRD results indicated that the cementation material in the biosandstone was a mixture of $Mg_5(CO_3)_4(OH)_2 \cdot 4H_2O$ and $MgNH_4PO_4(H_2O)_6$. Ammonia and ammonium could be converted into magnesium ammonium phosphate. Therefore, the biocomposite cement can
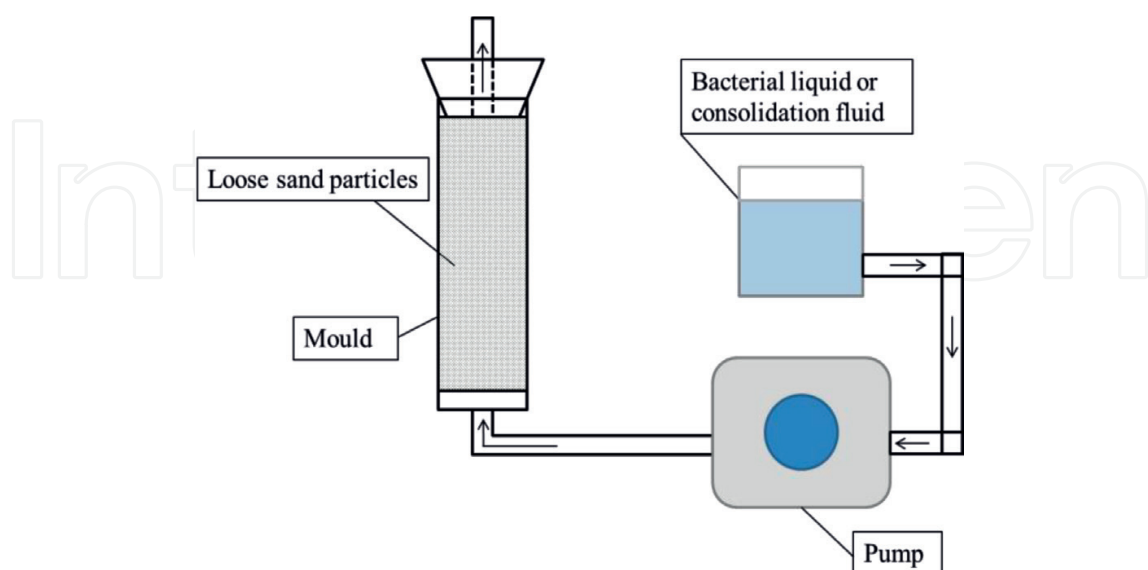

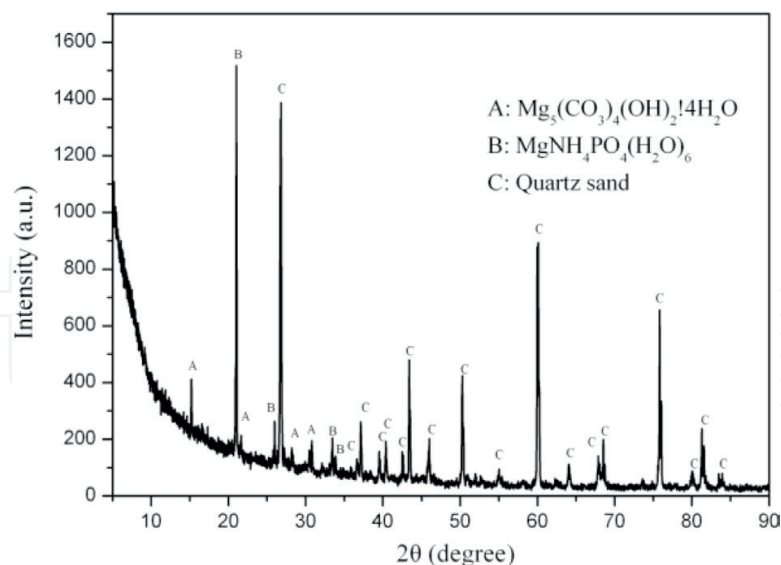**Figure 4.** Schematic diagram of biogrouting process [8].

Figure 5. X-ray diffraction of the biosandstone.

be synthesized through *Sporosarcina pasteurii*-induced precipitation. $MgNH_4PO_4(H_2O)_6$ was mainly prepared by magnesium ions reacting with ammonium and HPO_4^{2-} ions. Meanwhile, $Mg_5(CO_3)_4(OH)_2 \cdot 4H_2O$ could also be prepared by magnesium ions reacting with carbonate ions in the alkaline solution.

2.2.2. Influence of the number of injections on the hydraulic conductivity of sand columns

Figure 6 shows the hydraulic conductivity of the biosandstone. The average hydraulic conductivity of the sand was 3.97×10^{-2} cm/s before cementation. The average hydraulic conductivity of the biosandstone was 2.72×10^{-2}, 2.22×10^{-2}, and 2.03×10^{-2} cm/s when the number of injections was 2, 4, and 6, respectively. The hydraulic conductivity of the biosandstone decreased as the number of injections increased.

2.2.3. Influence of the number of injections on compressive strength and porosity of sand columns

Figure 7 shows the effect of the number of injections on compressive strength of the sand columns. When the number of injections increases from 2, 4, and 6, compressive strength of the sand columns increases sequentially, and the average compressive strength is 0.37, 0.80, and 1.53 MPa, respectively. After injecting 6 times, it is difficult to inject the biocomposite cement. Therefore, the maximum number of injections was 6 times. **Figure 8** shows the relationship between the number of injections and porosity. The average porosity of sand columns decreased from the initial 45.01 to 34.62, 29.55, and 25.15%, when CJ1, the number of injections was 2, 4, and 6, respectively, and the decrease rates were 10.39, 15.46, and 19.86%, respectively. The average porosity of sand columns shows a decrease with the increase in the number of injections.
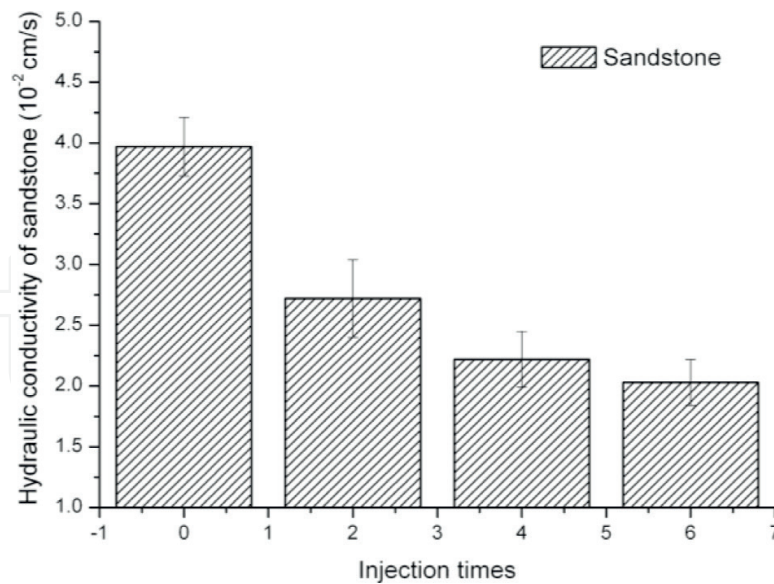
Figure 6. Effect of the number of injections on the hydraulic conductivity of the biosandstone.
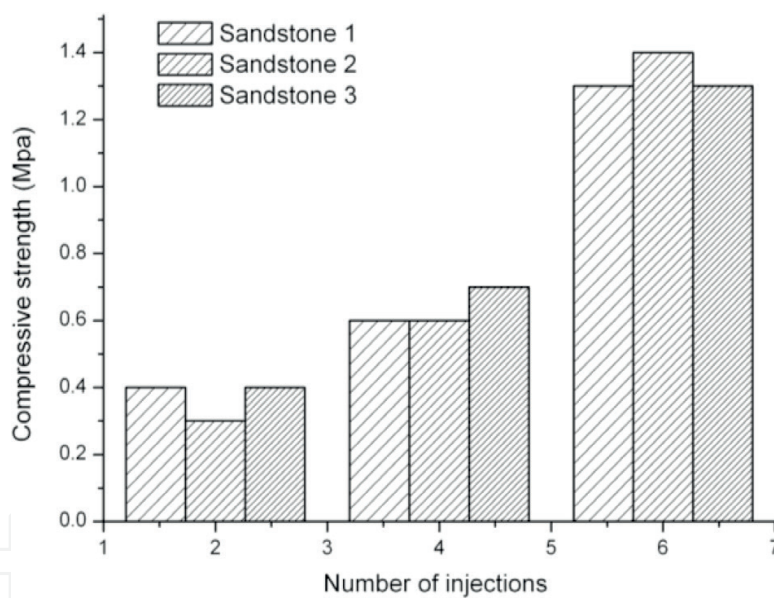

Figure 7. Effect of the number of injections on the compressive strength of sand columns.

2.2.4. Microstructure of sand columns under different number of injections

SEM images of sand columns with different number of injections are shown in **Figure 9**. **Figure 9(a–f)** shows the internal filling of the sand columns under numbers of injection 2, 4, and 6, respectively. The morphology of the particles is mainly an irregular sheet structure. **Figure 9(a, b)** shows that the internal filling of the sand column results in a small amount of composite cementitious material and cannot be filled in between the sand particles. **Figure 9(c, d)** shows that the interior of the sand column is filled, and the amount of the
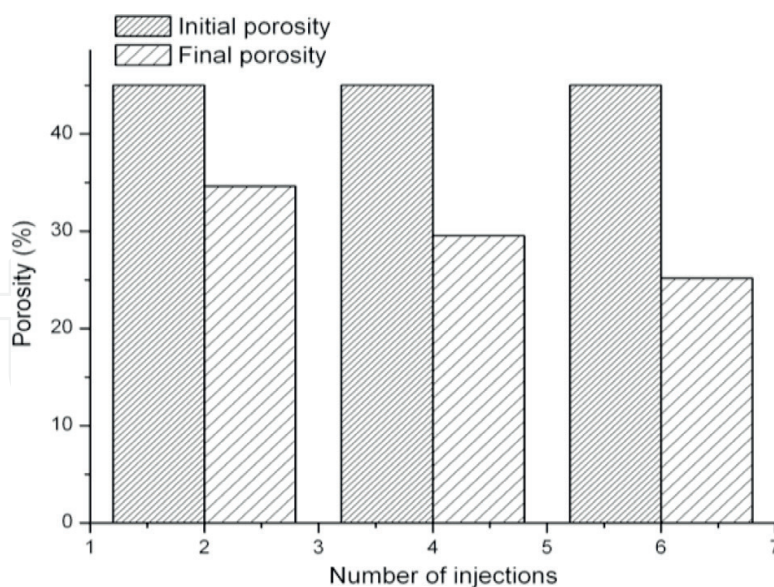
Figure 8. Effect of the number of injections on the porosity of sand columns.

composite cementitious material produced is more than **Figure 9(a, b)** and can be partly filled between the sand particles. **Figure 9(e, f)** shows that the interior of the sand column is well filled, and the amount of the composite cementitious material produced is more than that of 2 and 4 times. The loose sand grains could well be cemented into a whole with good mechanical properties. The above results also indicate that compressive strength, permeability, and porosity of the sand columns decrease with the increase in the numbers of injection.

2.2.5. 3D pore structure evolution of biosandstone produced using different number of injections

The XCT was Y. CT Precision S series high-precision computed tomography system from YXLON, Germany, with a resolution of micrometers. The test method was described in the literature [8]. XCT in situ trace tests were performed on sand columns with different cementation times (2, 4, and 6 times). The test results were analyzed using the defect analysis module in the VG Studio Max 2.0 software on the XCT device. According to the literature [9], VG Studio Max 2.0 software's defect analysis module and gray threshold algorithm are used to extract hole information, and a color scale is used to represent the size of the hole, in which blue to red represent from small holes to large holes. **Figure 10** shows the three-dimensional (3-D) pore structure evolution of the sand columns at different number of injections. When the number of injections increased, the defect volume in the sand columns gradually decreases. The maximum defect volume of the sand column with injecting 2 times was 1401 mm^3. After injecting 6 times, it decreased to 738 mm^3. This is due to the increase in the number of injections, resulting in more and more microbial cement product filling defects in the sand column. With the increase of the number of cementation, the size of the defect gradually decreased. This is also due to the increase in the number of
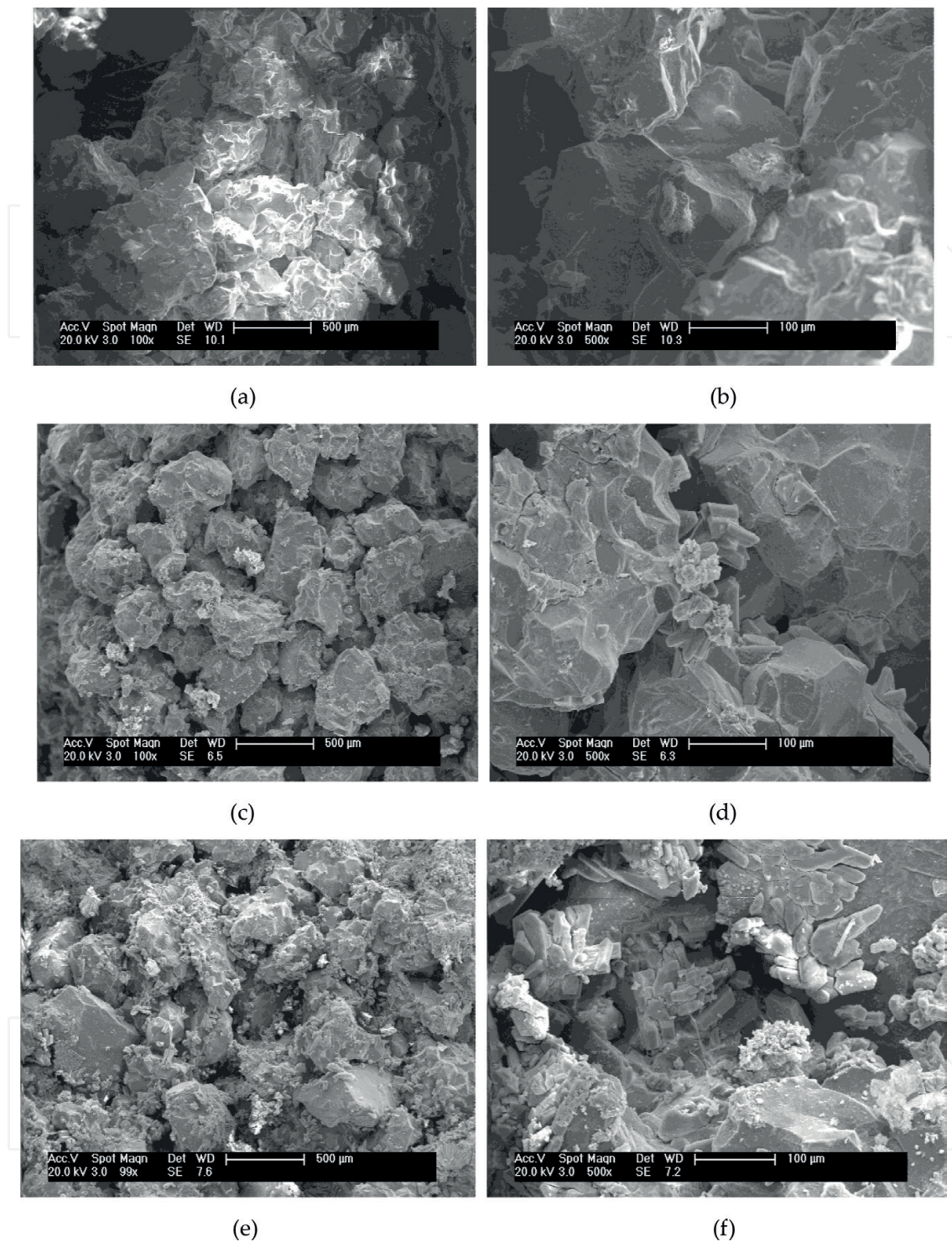
Figure 9. SEM images of sand columns: (a, b) 2 injections; (c, d) 4 injections; (e, f) 6 injections.

injections, resulting in the continuous filling of microbial cement in the defects, thereby reducing the size of defects and the number of defects. The overall defect distribution of the sand columns is not uniform. This is due to the inhomogeneity of defect distribution during the formation of loose sand grains, i.e., uneven distribution of internal defects, as
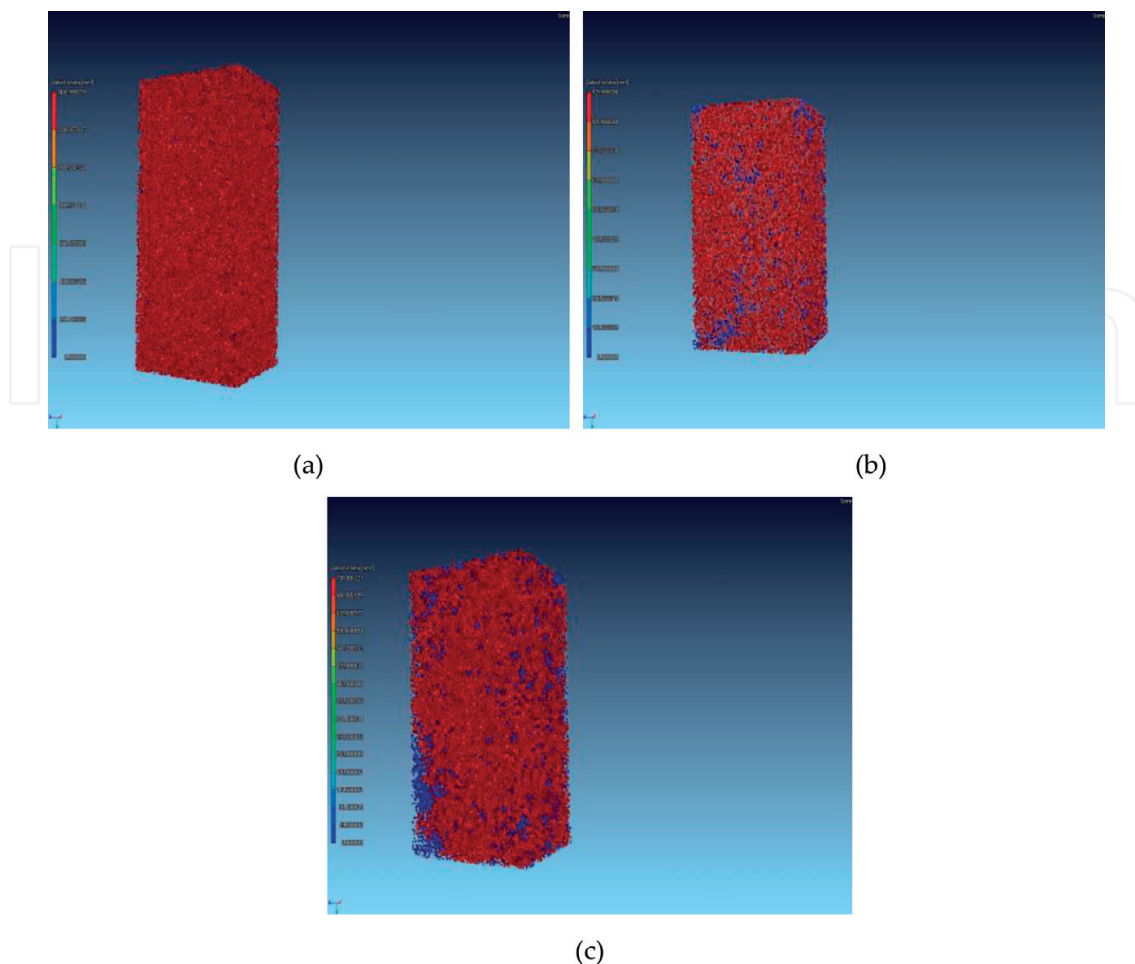
Figure 10. 3D pore structure evolution of biosandstone following: (a) 2 injections, (b) 4 injections, and (c) 6 injections.

shown in **Figure 10**. The average porosity of the sand columns was 36.20, 32.21, and 20.21% with corresponding injection times 2, 4, and 6, respectively. This result is similar to average porosity of 34.62, 29.55, and 25.15% for the sand columns measured at 2, 4, and 6 with paraffin drainage method.

3. Comparison of performance of sand columns cemented by biocomposite cement with preprecipitation mixing process and biogrouting process

By comparing the preprecipitation mixing process and the biogrouting process, the compressive strength of sand columns cemented by the preprecipitation mixing process sand column is poor, and the biogrouting process achieves a certain number of cementation can significantly improve the compressive strength, permeability, and porosity of sand columns. The reason

for the compressive strength of sand columns cemented by preprecipitation mixing process is inferior to the biogrouting process caused by the particle size and structure. For example, **Figure 3** shows that the particle morphology of the biocomposite cement is an irregular massive structure with a size in the range of 150–500 μm, while the pore size under tightly packed loose grains is less than 100 μm, resulting in the increase in the distance between sand grains under the preprecipitation mixing process. This is one of the reasons for the low compressive strength of the sand columns. Secondly, through the particle structure of the biocomposite cement, it can be judged that the bonding force between the particles is poor, which is also the reason why the compressive strength of sand columns is low. However, the particle size of the biocomposite cement formed by the grouting process is less than 100 μm, and the particles are tightly bound together in the sand columns, as shown in **Figure 9**. Therefore, it is better consolidate loose sand grains into a whole with good mechanical properties. In the next experiment, different formulations of biocomposite cement were used to cement loose grains under the grouting process, and the porosity, permeability, compressive strength, and internal microstructure of the sand columns were studied.

4. Different formulations of biocomposite cement binding loose sand

Each liter of solution for *Sporosarcina pasteurii* and $K_2HPO_4 \cdot 3H_2O$ (1, 1.5, and 2 mol/L) are named as CJ1, CJ1.5, and CJ2, respectively. Different types of magnesium ammonium phosphate and carbonate are synthesized by CJ1, CJ1.5, and CJ2 reacting with the mixture solution of $MgCl_2$ and urea (equimolar). Biocomposite cement was then obtained.

All sand columns were pared according to Section 2.2. All injection experiments were performed at room temperature of 25–30°C. PVC pipe (bottom of the cylinder) was connected with a peristaltic pump, and the CJ1, CJ1.5, and CJ2 and mixture solution of $MgCl_2$ and urea were injected from the bottom to top. The steps are as follows: (1) tap water was injected into three PVC pipes at a flow rate of 16 mL/min to exclude bubbles; (2) 100 mL of CJ1, CJ1.5, and CJ2 were injected to three PVC pipes, respectively; (3) injecting 100 mL of mixed solution of urea and $MgCl_2$ to PVC pipes standing for 6 h. The next steps are the same as in Section 2.2. Until CJ1, CJ1.5, and CJ2, mixed solution of urea and $MgCl_2$ could not be injected, and number of injections was 6, 4, and 3, respectively. Then, the specimens were placed in a 30 ± 2°C oven for curing for 15 days. The molds were removed and the corresponding sand columns were obtained. This method can well cement loose sand grains into a whole with mechanical properties, as shown in **Figure 11**. All tests were performed in triplicate and cemented at 30 ± 2°C. The initial porosity is 45.01 ± 2%.

4.1. XRD patterns of sand columns

The XRD diffraction peak of the sand column cemented by CJ1 was quartz (JCPDS No. 46-1045), $MgNH_4PO_4(H_2O)_6$ (JCPDS No. 71-2089), and $Mg_5(CO_3)_4(OH)_2 \cdot 4H_2O$ (JCPDS No.

25-0513) (**Figure 12(a)**). The XRD results show that the cementitious materials formed by CJ1 cementation sand column are mainly $MgNH_4PO_4(H_2O)_6$ and $Mg_5(CO_3)_4(OH)_2 \cdot 4H_2O$ complexes.

The XRD diffraction peak of the sand column cemented by CJ1.5 was quartz (JCPDS No. 86-2237), $MgNH_4PO_4(H_2O)_6$ (JCPDS No. 71-2089), $Mg_3(PO_4)_2(H_2O)_8$ (JCPDS No. 84-1148), and $MgCO_3(OH)_2(H_2O)_3$ (JCPDS No. 70-0591), as shown in **Figure 12(b)**. The XRD results show that the cementitious materials formed by CJ1.5 cement sand column are mainly $MgNH_4PO_4(H_2O)_6$ and $MgCO_3(OH)_2(H_2O)_3$ composites.

The XRD diffraction peak of the sand column cemented by CJ2 was quartz (JCPDS No. 89-1961), $MgNH_4PO_4 \cdot 6H_2O$ (JCPDS No. 15-0762), and $Mg_5(CO_3)_4(OH)_2 \cdot 5H_2O$ (JCPDS No. 23-1218) (**Figure 12(c)**). The XRD results showed that the cementitious materials formed by CJ2 cemented sand column were mainly $MgNH_4PO_4 \cdot 6H_2O$ and $Mg_5(CO_3)_4(OH)_2 \cdot 5H_2O$ complexes. The above results indicate that the main components of cementation product in sand columns are mainly magnesium ammonium phosphate (struvite) and hydromagnesite composites. Therefore, ammonia/ammonium (NH_3 /NH_4^+) can also be changed into struvite when *Sporosarcina pasteurii* contained $K_2HPO_4 \cdot 3H_2O$ in all cementation process.

4.2. Influence of different biocomposite cement on hydraulic conductivity of sand columns

Figure 13 indicates the influence on hydraulic conductivity of biosandstones by three different biophosphate and carbonate composite cements. The average hydraulic conductivity of the sand was 39.7×10^{-3} cm/s before cementation, as shown in **Figure 13(a)**. **Figure 13(b–d)** indicates that the average hydraulic conductivity of biosandstones cemented by CJ1, CJ1.5, and CJ2 is 20.3×10^{-3} cm/s, 2.52×10^{-3} cm/s, and 3.59×10^{-3} cm/s, respectively. Therefore, permeability of biosandstones can be retained when loose particles are cemented by three different biocomposite cements.
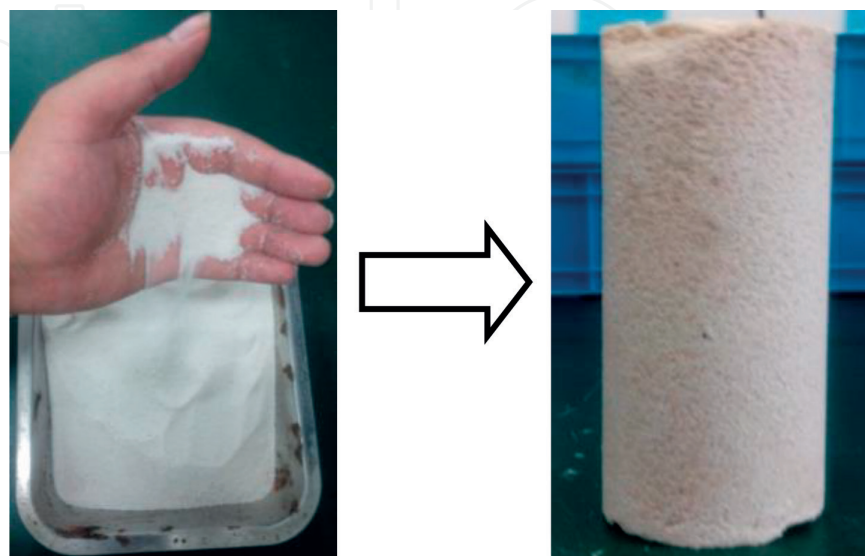

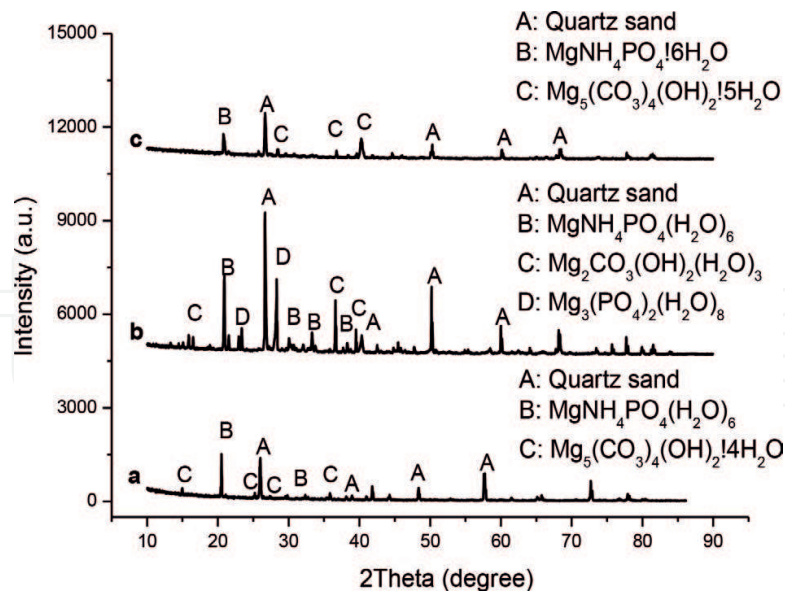**Figure 11.** Loose sand particles to sand column cemented by biocomposite cement.

Figure 12. X-ray diffraction of the sand columns cemented by three different biocomposite cements.

4.3. Influence of different biocomposite cement on compressive strength and porosity of sand columns

The effects of different biophosphate and carbonate composite cement on compressive strength are presented in **Figure 14**. **Figure 14(a–c)** shows that the average compressive strength of biosandstones cemented by CJ1, CJ1.5, and CJ2 are 1.53, 1.42, and 1.47 MPa, respectively. Results show that the maximum compressive strength of biosandstone cemented by CJ1 cementation is 1.59 MPa.

The relationship between average porosity and different biophosphate and carbonate composite cement is presented in **Figure 15**. The average porosity of biosandstones cemented by CJ1, CJ1.5, and CJ2 is effectively reduced from initial 45.01% down to 25.15%, 26.08%, and 25.87%, respectively, as shown in **Figure 15(a–c)**. The reductions were 19.86%, 18.93%, and 19.14%, respectively.
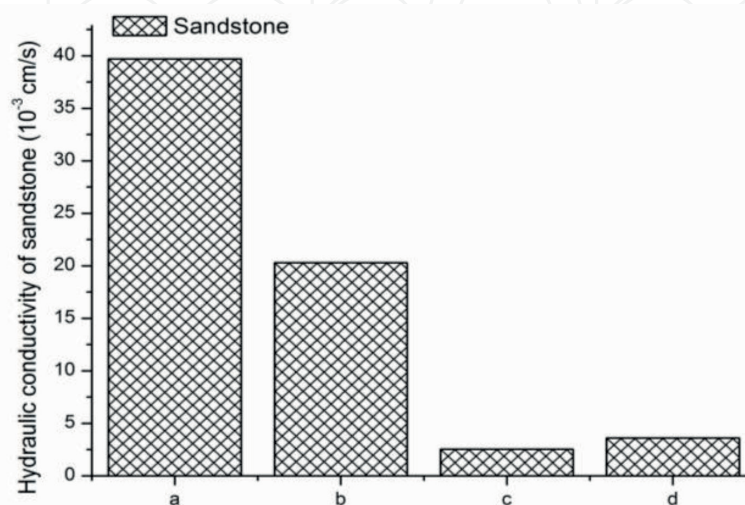

Figure 13. Effect of different biocomposite cement on the average hydraulic conductivity of sand columns.

4.4. Microstructure of sand columns cemented by different biocomposite cements

The SEM images of different formulations of biocement cemented sand columns are shown in **Figure 16**. **Figure 16(a, b)** shows the internal state of the CJ1 cemented sand column. The morphology of the composite cement product was mainly an irregular sheet structure and could be well filled between sand grains. The internal state of the CJ1.5 cemented sand column shows that the biocomposite cement product of morphology is an irregular particle cluster structure and can also be well filled between sand grains (**Figure 16(c, d)**). The internal state of the CJ2 cemented sand column shows that the morphology of the biocomposite cement product is also an irregular particle cluster structure, and can also be well filled between sand grains, as shown in **Figure 16(e, f)**. SEM images show that the porosity of sand columns can well be filled by three formulations of biocomposite cement.
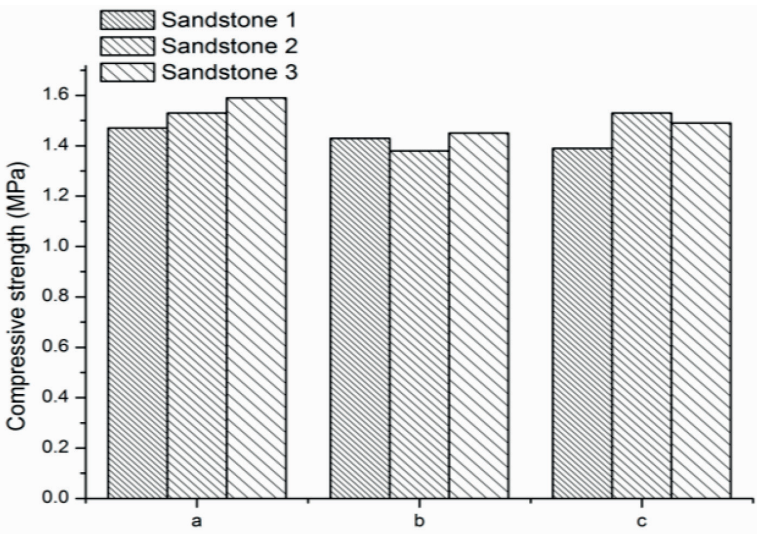

Figure 14. Effect of different biocomposite cements on compressive strength of sand columns.
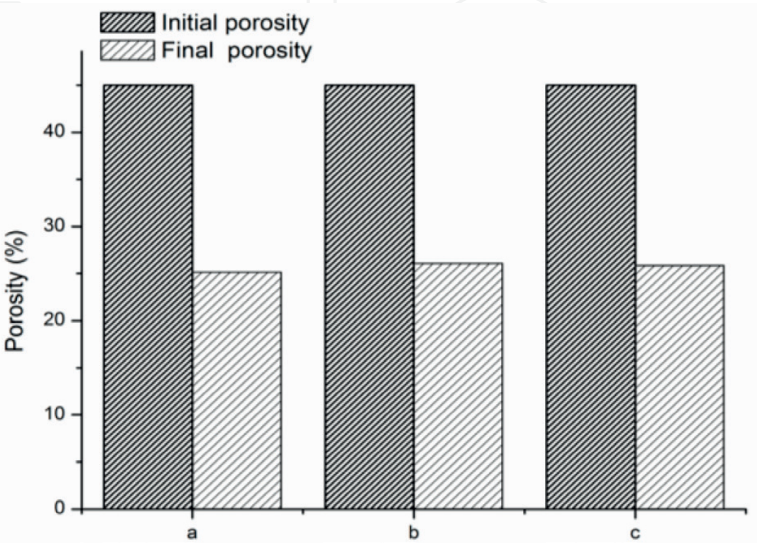

Figure 15. Effect of different biocomposite cements on the average porosity of sand columns.

4.5. Comparison of performance of three types of biocomposite cement

Above results show that the strength of sand columns cemented by three bio-composite cements is significantly lower than that of the biocarbonate cement bind sand columns. Similarly, three biocomposite cements can replace biocarbonate cement and can be applied to desert or dust treatment, sandy soil foundation, etc. The average permeability coefficients of sand columns cemented by CJ1, CJ1.5, and CJ2 were 2.03×10^{-3}, 2.52×10^{-2}, and 2.59×10^{-2} cm/s, respectively, and the average compressive strengths were 1.53, 1.42, and 1.47 MPa, respectively (**Table 2**). The content of biocomposite cement and compressive strength of sand columns are similar. The ammonia is released for 9.4, 7.5, and 5.7 g/L in CJ1, CJ1.5, and CJ2 cementation process, respectively. Therefore, CJ2 can effectively reduce ammonia emissions, and cementation numbers are least. Therefore, overall performance of CJ2 is optimum.
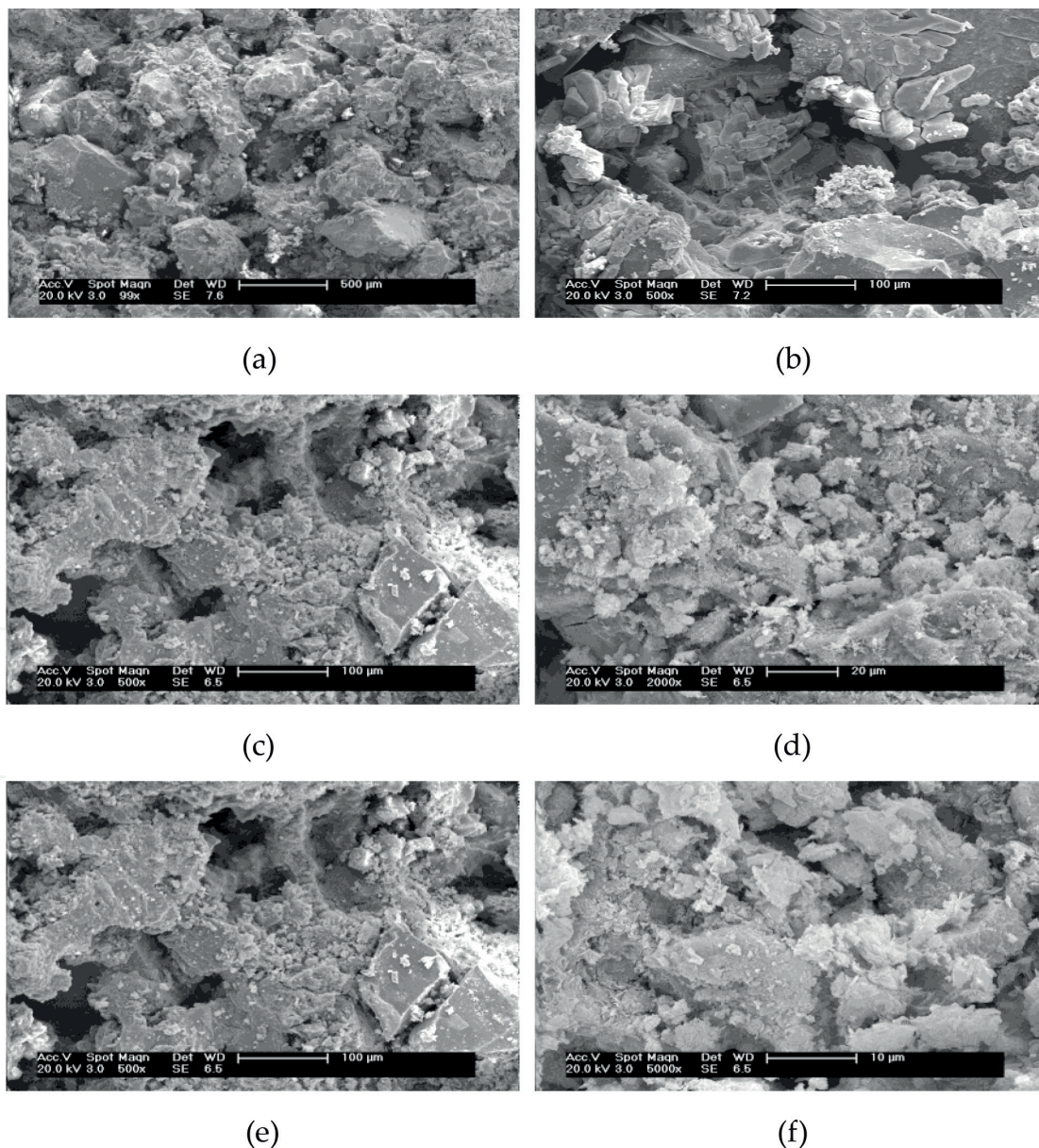

Figure 16. SEM images of the sand columns: (a, b) CJ1 cementation, (c, d) CJ1.5 cementation, and (e, f) CJ2 cementation.

5. Conclusions

Using biocomposite cement, loose sand grains can be cemented into sand columns with good mechanical strength by the biogrouting process. Ammonia was produced during the formation of biocarbonate cement and could be effectively become into struvite by phosphate. The number of injections has an important influence on the mechanical properties of sand columns. XRCT analysis showed that content of the biocomposite cement increased, the pores between sand grains gradually filled, and finally reducing the defect volume. Loose sand particles can well be cemented into biosandstone by three biocomposite cements. The performance of the biosandstones cemented by three formulations of composite cement was compared. Experiment results show that the compressive strength of sand columns cemented by three types of biocomposite cement is greater than 1.0 MPa. The weight of ammonia produced by CJ2 is less than CJ1 and CJ1.5.

Conflict of interest

The authors declare no conflict of interest.

Notes/thanks/other declarations

Author details

Xiaoniu Yu[1]* and Yan Gao[2]

*Address all correspondence to: xnyu@wzu.edu.cn

1 College of Civil Engineering and Architecture, Wenzhou University, Wenzhou, China

2 School of Continuing Education, Northeast Normal University, Changchun, China

References

[1] Qian CX, Yu XN, Wang X. A study on the cementation interface of bio-cement. Materials Characterization. 2018;**59**:1186-1193. DOI: 10.1016/j.matchar.2017.12.011

[2] Xiao P, Liu HL, Xiao Y, Stuedlein AW, Evans TM. Liquefaction resistance of bio-cemented calcareous sand. Soil Dynamics and Earthquake Engineering. 2018;**107**:9-19. DOI: 10.1016/j.soildyn.2018.01.008

[3] Terzis D, Laloui L. 3-D micro-architecture and mechanical response of soil cemented via microbial-induced calcite precipitation. Scientific Reports. 2018;**8**:1416. DOI: 10.1038/s41598-018-19895-w

[4] Azadi M, Ghayoomi M, Shamskia N, Kalantari H. Physical and mechanical properties of reconstructed bio-cemented sand. Soils and Foundations. 2017;**57**:698-706. DOI: 10.1016/j.sandf.2017.08.002

[5] Sari YD. Soil strength improvement by microbial cementation. Marine Georesources and Geotechnology. 2015;**33**:567-571. DOI: 10.1080/1064119X.2014.953234

[6] Salifu E, MacLachlan E, Iyer KR, Knapp CW, Tarantino A. Application of microbially induced calcite precipitation in erosion mitigation and stabilisation of sandy soil foreshore slopes: A preliminary investigation. Engineering Geology. 2016;**201**:96-105. DOI: 10.1016/j.enggeo.2015.12.027

[7] Yu XN, Qian CX, Xue B, Wang X. The influence of standing time and content of the slurry on bio-sandstone cemented by biological phosphates. Construction and Building Materials. 2015;**82**:167-172. DOI: 10.1016/j.conbuildmat.2015.02.038

[8] Yu XN, Qian CX, Sun LZ. The influence of the number of injections of bio-composite cement on the properties of bio-sandstone cemented by bio-composite cement. Construction and Building Materials. 2018;**164**:682-687. DOI: 10.1016/j.conbuildmat.2018.01.014

[9] Rong H, Qian CX, Li LZ. Study on microstructure and properties of sandstone cemented by microbe cement. Construction and Building Materials. 2012;**36**:687-694. DOI: 10.1016/j.conbuildmat.2012.06.063